

Multiresolution Decomposition of Areal Count Data

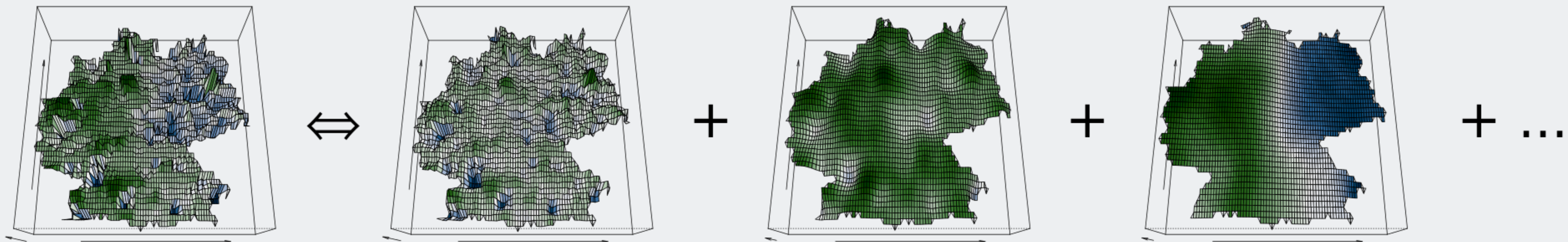
R. Flury^a, R. Furrer^{a,b}

^aDepartment of Mathematics; ^bDepartment of Computational Science, University of Zurich (Switzerland).

Contact: roman.flury@math.uzh.ch; @fluryro

Multiresolution Decomposition, an Image Processing Method to Answer:

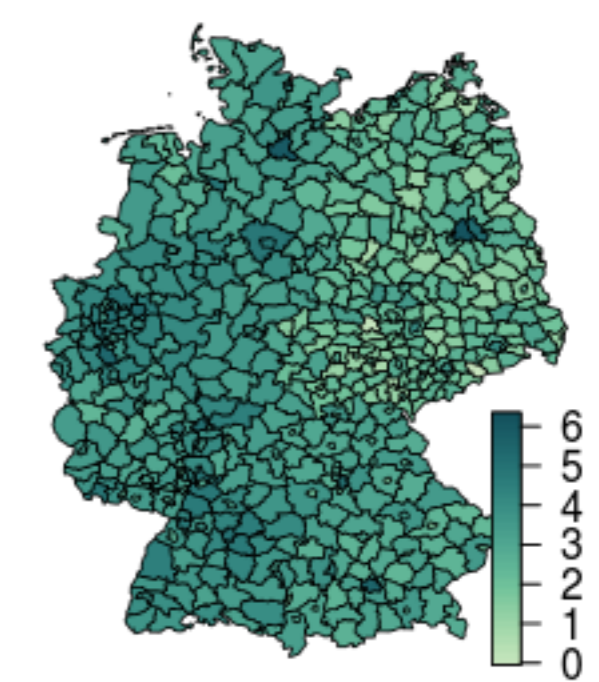
- Can we identify different features on different scales in regularly gridded data?
- Where are the predominant scale-dependent features located?



Rasterized areal count data.

Approach to Decompose Areal Count Data

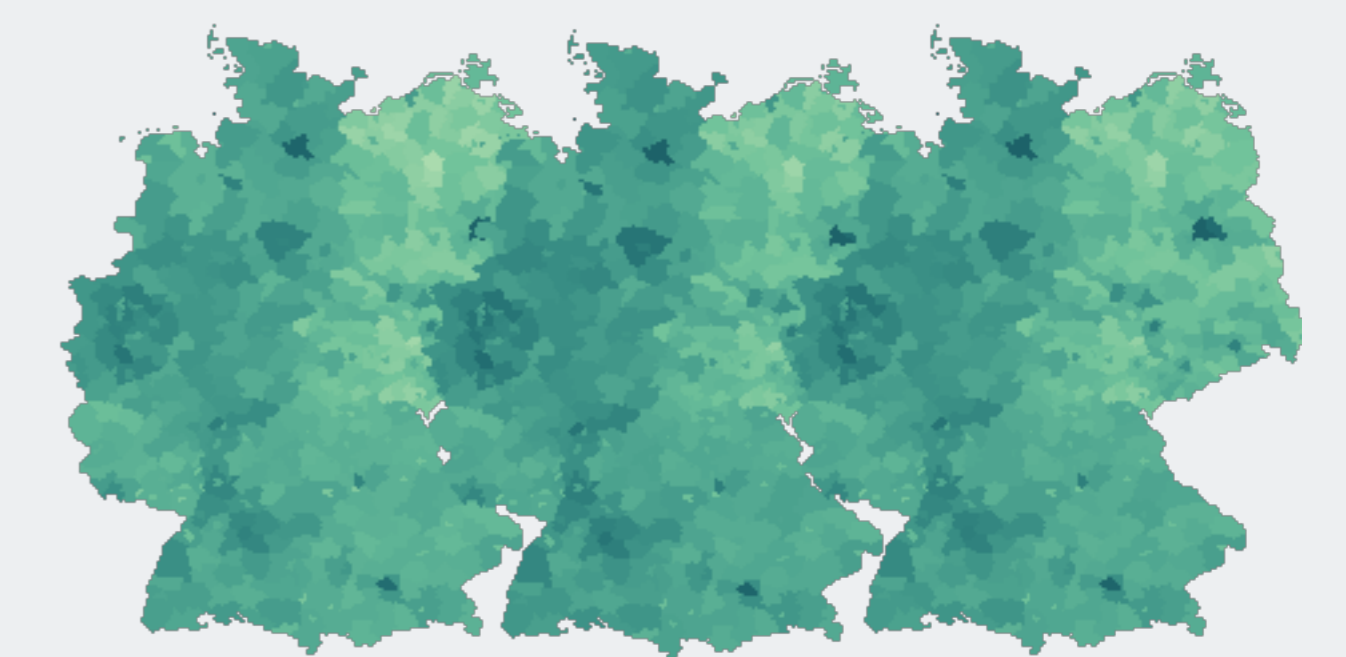
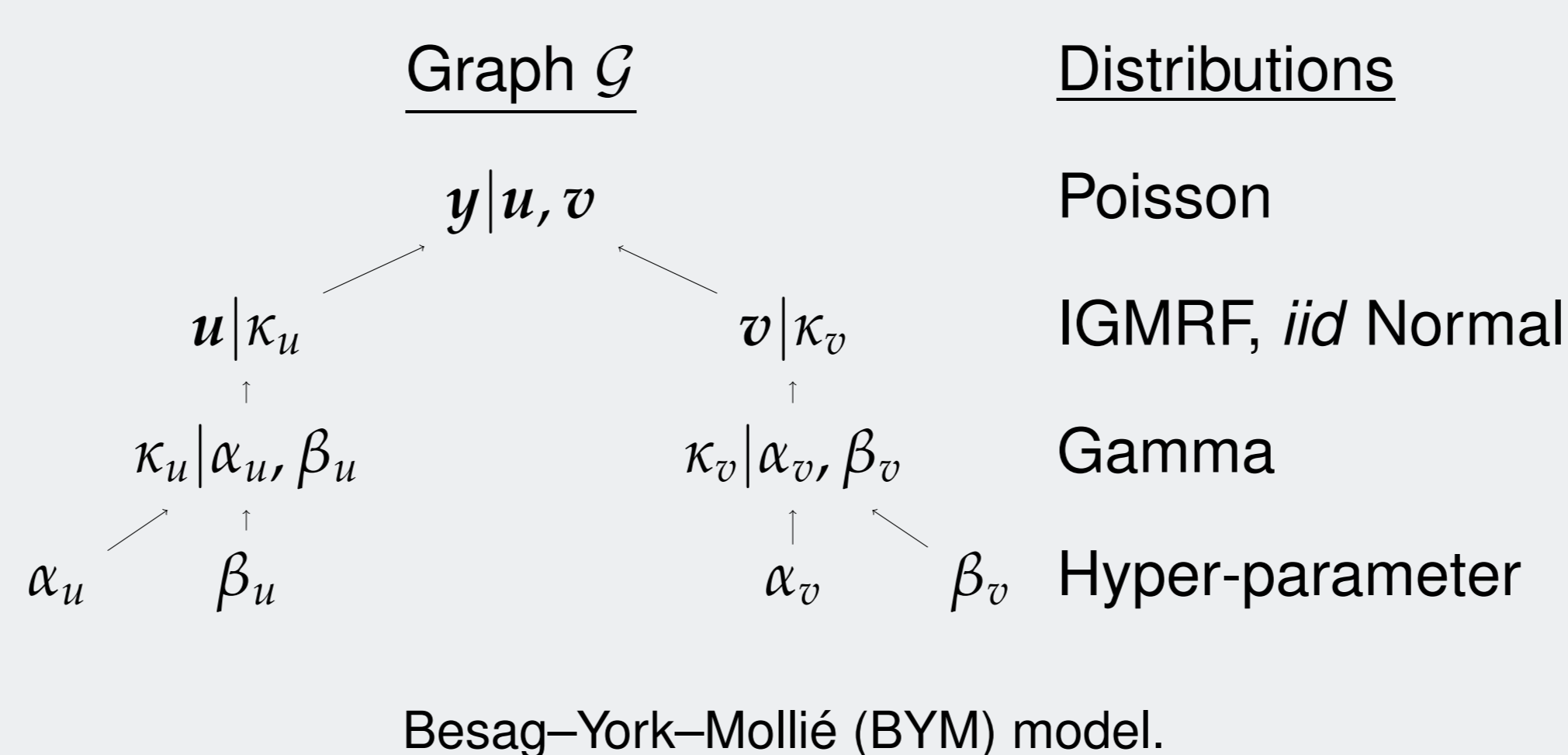
- Extending an image processing method¹ for incomplete, discrete and irregularly gridded data.
- Incorporating the Besag–York–Mollie model, to model count data and add a priori demographic knowledge.²
- Exploiting the sparse structure of the precision matrix for efficient computing.³
- Showing the method's feasibility on the oral cavity cancer log-counts per district in Germany.⁴
- The extended method consists of the three steps outlined below.



Oral cavity cancer log-counts in Germany. The counts were collected over 1986–1990.

1. Spatial Field Resampling

- Assume the observed field y compounds of the true field x and additive noise ε .
- Let y be the observed and e the known expected counts. The Poisson's rate is defined as $e \cdot \exp(u + v)$, where u is the spatially correlated log-relative risk and v a noise term.
- Resample u and v with a Metropolis-Hastings procedure.
- Reconstruct the log-counts with $e \cdot \exp(u + v)$, since the Poisson rate is equivalent to its mean.



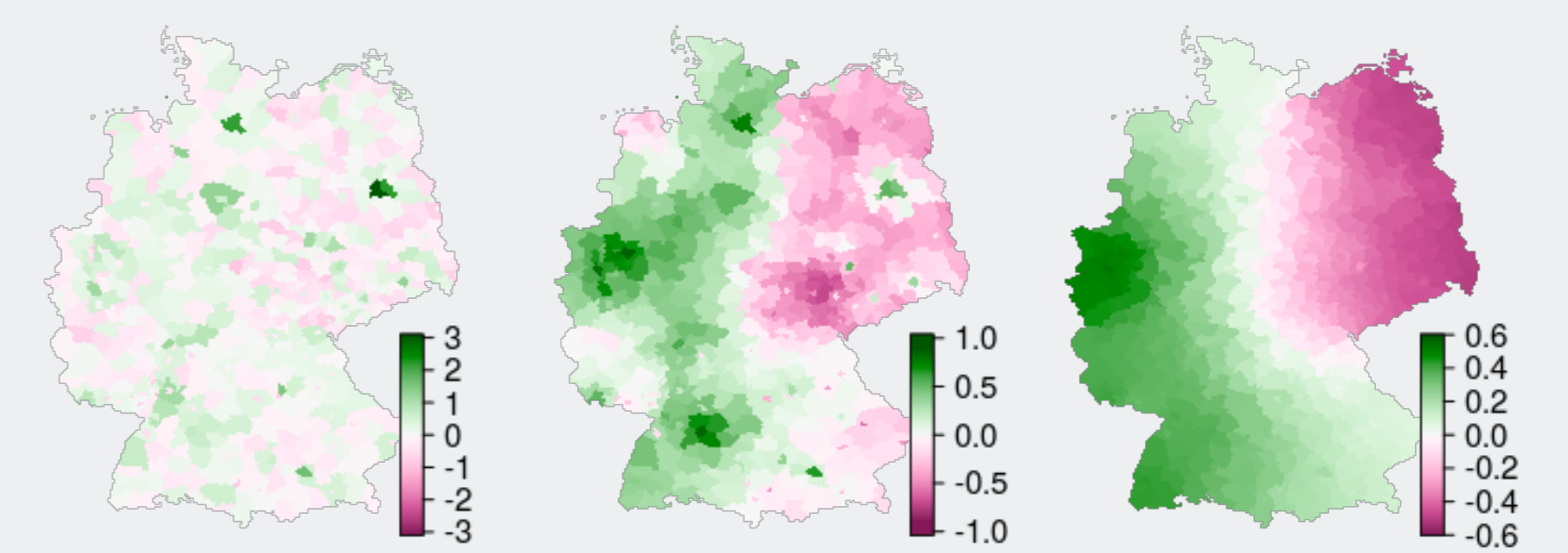
Reconstructed log-counts.

2. Calculating Differences Between Smooths

- We use a penalty smoother $S_\lambda = (\mathbf{I} + \lambda R)^{-1}$. R is the sparse precision matrix from the IGMRF (BYM model) based on adjacency relations. λ denotes the smoothing parameter such that $0 = \lambda_1 < \lambda_2 < \dots < \lambda_L = \infty$.
- The spatial field x can be written as differences of smooths, say details z_i ,

$$x = \sum_{i=1}^{L-1} (S_{\lambda_i} x - S_{\lambda_{i+1}} x) + S_{\lambda_L} x = \sum_{i=1}^L z_i.$$

- λ 's are chosen such that the differences between smooths are maximal.



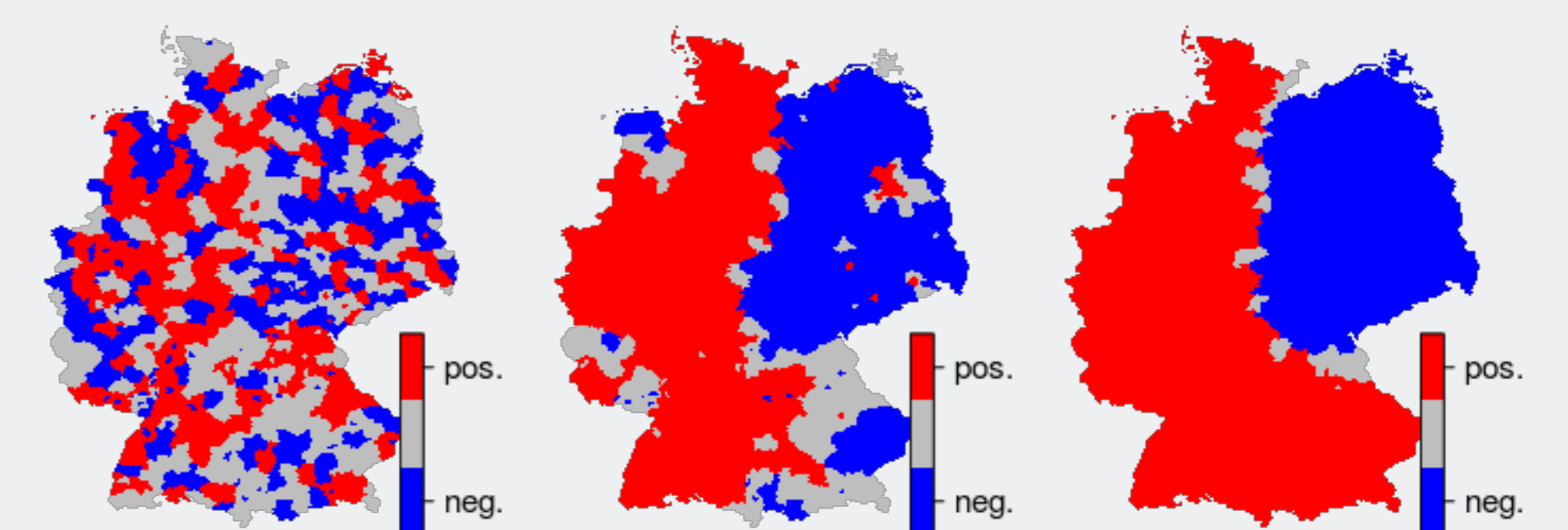
Scale dependent details summarized by their posterior means: $E(z_1|y)$, $E(z_2|y)$ and $E(z_3|y)$ (left to right).

3. Credibility Analysis

In pointwise probability maps, for each detail z_i , the locations s are divided into three different subsets in which the components $z_{i,s}$ differ jointly credible from zero, with credibility level $\alpha = 95\%$.

$$I^{\text{blue}} = \{s | P(z_{i,s} > 0 | \text{data}) \geq \alpha\}, \quad I^{\text{red}} = \{s | P(z_{i,s} < 0 | \text{data}) \geq \alpha\} \quad \text{and} \quad I^{\text{gray}} = I \setminus (I^{\text{blue}} \cup I^{\text{red}}).$$

The corresponding maps indicate with blue jointly credible negative and with red jointly credible positive areas.



Pointwise probability maps for details z_1 , z_2 and z_3 (left to right).

References

- ¹Holmström L., Pasanen L., Furrer R., Sain S. R. (2011). Scale space multiresolution analysis of random signals. *Computational Statistics & Data Analysis* **55**, 2840–2855.
- ²Besag J., York J., Mollie A. (1991). Bayesian image restoration, with two applications in spatial statistics. *Annals of the Institute of Statistical Mathematics* **43**, 1–20.
- ³Furrer R., Sain S. R. (2010). A sparse matrix R package with emphasis on MCMC methods for Gaussian Markov random fields. *Journal of Statistical Software* **36**, 1–25.
- ⁴Knorr-Held L., Raßer G. (2000). Bayesian detection of clusters and discontinuities in disease maps. *Biometrics* **56**, 13–21.